

## THE DEPOSITION OF CuInSe<sub>2</sub> LAYER ON GLASS SUBSTRATE BY SILAR METHOD

A. IVANAUSKAS, R. IVANAUSKAS, I. ANCUTIENE

*KTU, Department of Physical and Inorganic Chemistry, Radvilenu pl. 19, LT-50254 Kaunas*

The copper indium selenide (CuInSe<sub>2</sub>) layer was successfully deposited on glass substrate via the successive ionic adsorption and reaction (SILAR) method. The layer has been deposited in three steps and then was annealed for 12 hours under nitrogen atmosphere at 100° C. Diseleniumtetrathionate (H<sub>2</sub>Se<sub>2</sub>S<sub>2</sub>O<sub>6</sub>) acid solution was used as the selenization precursor. The solid intermediates obtained at different steps of layer deposition process was investigated in detail by X-ray diffraction analysis (XRD) and X-ray photoelectron spectroscopy (XPS) in order to understand the reaction pathway. XRD and XPS data showed that the annealing process for successful layer of copper indium selenide formation is necessary and the layer deposition phases sequence was Se → Cu<sub>x</sub>Se → mixture of phases → CuInSe<sub>2</sub>. Based on experiment results, the possible reactions that take place during the process of layer formation have been proposed.

(Received July 8, 2016; ; Accepted August 23, 2016)

**Keywords:** selenopolythionates, selenium, chalcogenides, SILAR, XRD, XPS

### 1. Introduction

Solar cells are one of the most prominent and promising energy technology today. It is not only sustainable, but also, renewable, clean, completely noise free, scalable, minimal amount of maintenance is required and it produces zero emissions.

CuInSe<sub>2</sub> is one of many potentially efficient materials for solar cell applications. Among these, it exhibits great optical absorption coefficient ( $>10^5 \text{ cm}^{-1}$ ) [1, 2], low direct band gap (1.04 eV) [2] and high thermal resilience [3]. Also, these optical properties do not get worse under highly intense irradiation[4]. Today, CuInSe<sub>2</sub> layers can reach 20.5% efficiency, while in solar cell 18.7% [5].

CuInSe<sub>2</sub> layers can be obtained using chemical or physical deposition. These methods include chemical vapor deposition[6], spin-coating [7,8], electrochemical deposition [2,3,9], chemical bath deposition(CBD)[10]. Physical deposition methods include sputtering [11], molecular beam epitaxy [12], electron beam evaporation[13,14], printing [15,16] and others. These methods, on the other hand, offers better quality layers, while often requiring high cost low-pressure, high-temperature equipment and it does not offer good scalability for large area coating. Physical deposition techniques often require annealing in H<sub>2</sub>Se atmosphere, which results in reagent wastage, even lower cost efficiency and toxic work environment[9]. In regards to electrochemical deposition, it is rather difficult to co-deposit three elements (Cu, In, Se) simultaneously with widely spread redox potentials. Often, unwanted non stoichiometric Cu<sub>2-x</sub>Se phase is formed that degrades layer's properties. Another downside for electrochemical deposition is the formation of non-conductive hydroxides on cathode. Various organic solvents can be added to avoid this, neglecting health hazard free environment. Sol-gel method is not a subject to this [9]. Thus, chemical deposition methods could be most convenient way to deposit CuInSe<sub>2</sub>, by avoiding hazardous selenization process. SILAR method is presently attracting considerable attention, as it does not require sophisticated instrumentation like vacuum system and other expensive equipment.

\*Corresponding author: algimantas.ivanauskas.88@gmail.com

Simple equipment like hot plate with magnetic stirrer is needed. The starting chemicals are commonly available and cheap. By using this method homogeneous layers are formed and it is easy scalability for large surface area coatings. However, it usually requires annealing to obtain crystalline CuInSe<sub>2</sub> layer [1].

The present work brings a complete study on the deposition of CuInSe<sub>2</sub> and In<sub>2</sub>Se<sub>3</sub> layer using SILAR method in a three steps process and annealing in nitrogen atmosphere. To understand the reaction pathway of CuInSe<sub>2</sub> layer its composition was investigated through X-ray diffraction and X-ray photoelectron spectroscopy measurements.

## 2. Experimental

### 2.1. CuInSe<sub>2</sub> layer deposition

The glass substrates were used 20 mm × 20 mm × 1 mm with a matte finish on a single side. All substrates were washed with liquid soap and distilled water and dried. Then they were cleaned in ultrasonically in acetone bath for 10 min at 40 °C. The CuInSe<sub>2</sub> layer was deposited in three steps plus annealing. First, selenium layer was formed by submerging glass substrate into 0.4 M H<sub>2</sub>SeO<sub>3</sub> and 1 M KHSO<sub>3</sub> 1:1 mixture at 60 °C for three hours. Then the sample was rinsed with distilled water and was placed for 10 min in solution of 0.4 M CuSO<sub>4</sub> with addition of 1% hydroquinone at 60 °C. It is a mixture of univalent and divalent copper salts consisting of 0.34 M Cu(II) and 0.06 M Cu(I) salt. Next, it rinsed with distilled water and was submerged in 0.1 M InCl<sub>3</sub> solution for 10 min at 40 °C. Lastly, the sample was dried over CaCl<sub>2</sub> for 24 h and was annealed 12 h in inert nitrogen atmosphere at 100 °C.

Potassium hydrosulphite (KHSO<sub>3</sub>) (≥98.0% from Sigma–Aldrich), selenous acid (H<sub>2</sub>SeO<sub>3</sub>) (99.999% trace metals basis from Aldrich), crystalline copper sulphate pentahydrate (CuSO<sub>4</sub>·5H<sub>2</sub>O) (crystals and lumps, 99.999% trace metals basis, from Sigma–Aldrich), and hydroquinone (C<sub>6</sub>H<sub>4</sub>(OH)<sub>2</sub>) (flakes, ≥99% Reagent Plus® from Sigma–Aldrich) and indium (III) chloride (InCl<sub>3</sub>) (reagent grade, 98%, powder from Sigma–Aldrich) for experiments were used.

### 2.2. XRD characterization

X-ray diffraction analysis of the layers deposited on glass substrate surface after each step was performed using a D8 Advance diffractometer (Bruker AXS, Karlsruhe, Germany) operating at the tube voltage of 40 kV and tube current of 40 mA. Diffraction patterns were recorded in a Bragg-Brentano geometry using a fast counting 1-dimensional detector Bruker Lynx Eye based on silicon strip technology. The X-ray beam was filtered with Ni 0.02 mm filter to suppress Cu-K $\alpha$  radiation and specimens were scanned over the range  $2\theta = 3\text{--}70^\circ$  at a scanning speed of 6°/min using a coupled two theta/theta scan type. Diffractometer is supplied together with software package DIFFRAC.SUITE. X-ray diffractograms of deposited layers were processed using the software packages Search Match, ConvX, Xfit and Microsoft Office Excel.

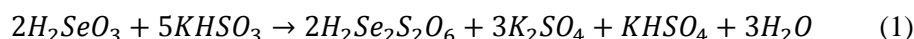
### 2.3. XPS characterization

XPS measurements were carried out to obtain information about the elemental chemical states and surface composition of the layers deposited on glass substrate surface on the upgraded Vacuum Generator (VG) ESCALAB MKII spectrometer fitted with a new XR4 twin anode. The non-monochromatised MgK $\alpha$  X-ray source was operated at  $h\nu = 1253.6$  eV with 300 W power (20 mA/15 kV) and the pressure in the analysis chamber was lower than  $5 \times 10^{-7}$  Pa during spectral acquisition. The spectra were acquired with an electron analyser pass energy of 20 eV for narrow scans and resolution of 0.05 eV and with a pass energy of 100 eV for survey spectra. All spectra were recorded at a 90° take-off angle and calibrated from the hydrocarbon contamination using the C 1s peak at 284.6 eV. The spectra calibration, processing and fitting routines were done using Advantage software (5.918) provided by Thermo VG Scientific. Core level peaks of Se 3d, Cu 2p, In 3d, O 1s, Cl 2p and Cl 1s were analysed using a nonlinear Shirley-type background and the calculation of the elemental composition was performed on the basis of Scofield's relative sensitivity factors. The layer surface was sputtered by Ar<sup>+</sup> ions having the energy of 2 keV and duration of 15 s.

### 3. Results and discussion

#### 3.1. The formation mechanism of $\text{In}_2\text{Se}_3$ and $\text{CuInSe}_2$ layer on glass substrate

The glass substrates with a matte finish on a single side for formation the  $\text{In}_2\text{Se}_3$  and  $\text{CuInSe}_2$  layer on its surface were used. A three-step mechanism of this layer can be proposed. In the first step selenium layer was formed by submerging glass substrate into mixture solutions of  $\text{H}_2\text{SeO}_3$  and  $\text{KHSO}_3$ . The components of mixture react with each other and the acid of diselenium tetrathionate in solution according to reaction is formed[17]:



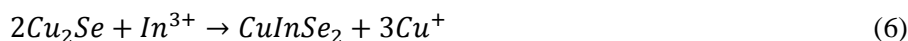
$\text{H}_2\text{Se}_2\text{S}_2\text{O}_6$  then decomposes and releases elemental selenium, which is deposited on glass substrate [18]:



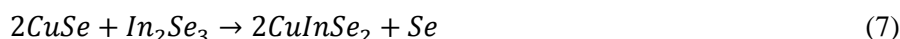
During next step the glass substrates with selenium layer was placed to solution of  $\text{CuSO}_4$  with hydroquinone. The elemental selenium on glass substrate is reacted with  $\text{Cu(I)}$  ions and  $\text{Cu}_x\text{Se}$  layer formation proceeds according to reaction:



In the next step the glass substrates with the layer of copper selenide was treated with solution of  $\text{InCl}_3$ . Possible formation reactions of  $\text{In}_2\text{Se}_3$  layer are:



An exchange of ions is possible because the solubility product for  $\text{In}_2\text{Se}_3$  is  $5.6 \times 10^{-92}$ , whereas for  $\text{CuSe}$  and  $\text{Cu}_2\text{Se}$  the solubility products are  $1.4 \times 10^{-36}$  and  $1.1 \times 10^{-51}$ , respectively [19]. Lastly, the samples were annealed in inert (nitrogen) atmosphere at  $100^\circ\text{C}$ . Possible solid-state reactions are these:



Formation of  $\text{CuInSe}_2$  layer on glass substrate during the reactions (1) through (8) result in change of the glass substrate colour from transparent through red to dark grey, as shown in Fig. 1.

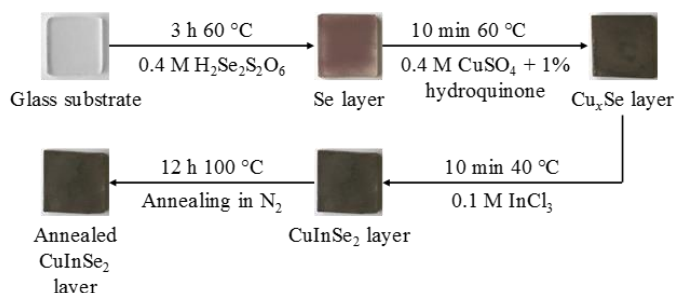


Fig. 1. Schematics of  $\text{CuInSe}_2$  layer on glass substrate synthesis procedure

Nevertheless, to make sure that the layer of  $\text{CuInSe}_2$  on glass substrate was formed this layer requires further investigation. To understand the reaction pathway of  $\text{CuInSe}_2$  on glass substrate by SILAR method, the solid intermediates obtained at different stages of synthesis process were investigated in detail by XRD and XPS methods.

### 3.2. XRD analysis

The Fig.2 shows XRD patterns of solid intermediates and  $\text{CuInSe}_2$  layers on the glass substrate obtained on different steps of their formation process. It can be seen that there are clear characteristic peaks of the layers on all four patterns. When the glass substrate was submerged into mixture of solutions  $\text{H}_2\text{SeO}_3$  and  $\text{KHSO}_3$  at  $60^\circ\text{C}$  for three hours (pattern (a)), only one peak (+) at  $2\theta = 23.5^\circ$  phase of monoclinic selenium (JCPDS: 24-714) appears (Table 1). Only single selenium peak indicates that majority of selenium is in amorphous phase, which is red color. It is known, that amorphous selenium is more active than black crystalline selenium [20]. That is why amorphous selenium should react more actively with copper ions.

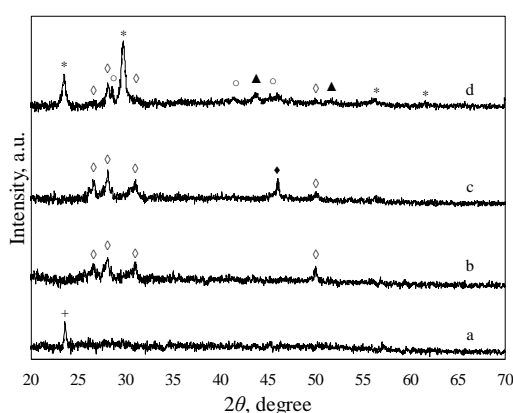


Fig. 2. XRD patterns of solid intermediates and  $\text{CuInSe}_2$  layers on the glass substrate obtained on different steps of their formation process: (a) the deposition layer of selenium; (b) the formation layer of  $\text{Cu}_x\text{Se}$ ; (c) the formation layer of  $\text{CuInSe}_2$ ; (d) the annealing layer of  $\text{CuInSe}_2$ . Peaks were identified and assigned as follows: (+) – Se (24-714) monoclinic selenium; (\*) – Se (73-465) hexagonal selenium; (◇) –  $\text{Cu}_{0.87}\text{Se}$  (83-1814) hexagonal klockmanite; (◆) –  $\text{In}_2\text{Se}_3$  (20-492) cubic indium selenide; (○) –  $\text{In}_2\text{Se}_3$  (17-356) indium selenide; (▲) –  $\text{CuInSe}_2$  (23-207) cubic copper indium selenide.

This pattern confirms the (1) and (2) equations of reactions which take place during first step when layer of selenium on the glass substrate was formed. When the glass substrate with layer of selenium was submerging into solution of  $\text{CuSO}_4$  with hydroquinone, the peak corresponding to phase of monoclinic selenium on pattern (b) disappears, but the four peaks (◇) at  $2\theta = 26.6, 28.1, 31.1$  and  $50.0^\circ$  of copper selenide phase – hexagonal klockmannite  $\text{Cu}_{0.87}\text{Se}$  (JCPDS: 83-1814) appear (Table 1). The disappearance phase of monoclinic selenium and the appearance phase of copper selenide indicated that the reaction of the formation of  $\text{Cu}_x\text{Se}$  which was described in equation of (3) had taken place. When the glass substrate with layer of copper selenide was submerging into solution of  $\text{InCl}_3$ , one peak (◆) at  $2\theta = 46.0^\circ$  phase of cubic indium selenide  $\text{In}_2\text{Se}_3$  (JCPDS: 20-492) appears (pattern (c)) (Table 1). It indicates the formation of new phase of indium selenide according equations (4) and (5). Therefore, the intensively and clear characteristic peaks of the  $\text{Cu}_{0.87}\text{Se}$  in the XRD pattern (c) show that the layer formed after third step consists of only  $\text{Cu}_{0.87}\text{Se}$  phase and a little amount of  $\text{In}_2\text{Se}_3$  phase. Looking at our results, we see, that annealing is needed to obtain  $\text{CuInSe}_2$  phase. Finally, sample was annealed 12 h in the inert (nitrogen) atmosphere at  $100^\circ\text{C}$ . Then on the XRD pattern (d) in Fig. 2 of annealed layer can be seen noticeable big changes. The intensities of four diffraction peaks of hexagonal klockmannite  $\text{Cu}_{0.87}\text{Se}$  markedly decrease and the diffraction peak of cubic indium selenide disappears. It should be noted that two intensive diffraction peaks (\*) at  $2\theta = 23.5, 29.7^\circ$  and two

weak diffraction peaks at  $56.3^\circ$  and  $61.7^\circ$  of new phase of hexagonal selenium (JCPDS: 73-465) can be clearly observed. Meanwhile accompanying with two weak diffraction peaks ( $\blacktriangle$ ) at  $43.6^\circ$  and  $51.8^\circ$  of phase of cubic copper indium selenide (JCPDS: 23-207) and three diffraction peaks ( $\circ$ ) at  $28.6^\circ$ ,  $41.3^\circ$  and  $45.3^\circ$  of new phase of indium selenide (JCPDS: 17-356). These detected results definitively can be illustrated by solid-state reactions which were described in equations (7) and (8), when phases of hexagonal selenium (JCPDS: 73-465) and copper indium selenide (JCPDS: 23-207) were formed. In addition, as a result of these reactions, the amount of phase of copper selenide  $\text{Cu}_{0.87}\text{Se}$  (JCPDS: 83-1814) decreases significantly and phase of indium selenide  $\text{In}_2\text{Se}_3$  (JCPDS: 20-492) disappears completely.

This confirms the mentioned above variation intensities of diffraction peaks attributed to the following phases in the XRD pattern (d). It is possible that selenium and cation of univalent copper had formed during reactions (5), (6) and (7) react with each other and according to equation (3) and copper selenide is formed. Then copper selenide react with cations of  $\text{In}^{3+}$  according to equations (4) and (5) and the phase of indium selenide (JCPDS: 17-356) formed.

*Table 1. XRD  $2\theta$  peaks and their assignment of  $\text{CuInSe}_2$  layer on glass substrate formed by SILAR method.*

Stage of layer formation	Symbol in Fig. 1 – crystallographic phase (JCPDS file number): peak positions $2\theta$ , degrees
Step 1	(+) – Se (24-714): 23.52
Step 2	( $\diamond$ ) – $\text{Cu}_{0.87}\text{Se}$ (83-1814): 26.62, 28.11, 31.08, 50.00
Step 3	( $\diamond$ ) – $\text{Cu}_{0.87}\text{Se}$ (83-1814): 26.62, 28.11, 31.08, 50.00 ( $\blacklozenge$ ) – $\text{In}_2\text{Se}_3$ (20-492): 46.05
After annealing	(*) – Se (73-465): 23.52, 29.70, 56.25, 61.67 ( $\blacktriangle$ ) – $\text{CuInSe}_2$ (23-207): 43.61, 51.78 ( $\circ$ ) – $\text{In}_2\text{Se}_3$ (17-356): 28.57, 41.32, 45.30 ( $\diamond$ ) – $\text{Cu}_{0.87}\text{Se}$ (83-1814): 26.62, 28.11, 31.08, 50.00

### 3.3. XPS analysis

In order to get more information about the formation of  $\text{CuInSe}_2$  layer on the glass substrate it was analyzed by X-ray photoelectron spectroscopy (XPS). The surface of layer obtained, when the glass substrate was submerged into mixture of solutions  $\text{H}_2\text{SeO}_3$  and  $\text{KHSO}_3$  (first step), and the surface of  $\text{CuInSe}_2$  layer and its deeper areas after etching (up to 20  $\mu\text{m}$ ) were studied. The signal of a freshly prepared selenium layer shown in Fig 3 Se3d region, curve (c) exhibits a signal at 55.70 eV which corresponds to the selenium in elemental state ( $\text{Se}^0$ ) [21]. The high resolution XPS spectra of  $\text{CuInSe}_2$  layer in Cu2p, In3d and Se3d regions are also shown in Fig. 3 curves (a). For surface layer of  $\text{CuInSe}_2$ , the binding energy (BE) of  $\text{Cu}2p_{3/2}$  and  $\text{Cu}2p_{1/2}$  is 932.33 eV and 952.58 eV respectively, which is consistent with BE values of  $\text{CuInSe}_2$  [22] and  $\text{Cu}_2\text{Se}$  or  $\text{Cu}_2\text{O}$  [23,24]. The BE value of 55.18 eV for the  $\text{Se}3d_{5/2}$  level is assigned to the  $\text{CuInSe}_2$  [22] and elemental Se [25]. The predominant features of  $\text{InCl}_3$  exhibiting BE of 445.91 eV and 454.03 eV for the  $\text{In}3d_{3/2}$  and  $\text{In}3d_{5/2}$  levels [26,27].

The high resolution XPS spectra of etched layer of  $\text{CuInSe}_2$  in Cu2p, In3d and Se3d regions are shown in Fig. 3 curves (b). The BE of XPS peaks corresponding to levels Cu2p and Se3d ( $\text{Cu}2p_{3/2}$  at 932.33 eV,  $\text{Cu}2p_{1/2}$  at 952.58 eV and  $\text{Se}3d_{5/2}$  at 55.18 eV) are not changed and indicates that compound composition remains unchanged deeper than 20  $\mu\text{m}$  from surface.

However, the both peaks of BE of  $\text{In}3d_{3/2}$  and  $\text{In}3d_{5/2}$  for etched layer shifted to direction of lower BE than that of non-etched surface of layer. The BE of  $\text{In}3d_{5/2}$  is 445.10 eV respectively, which is consistent with BE values of  $\text{In}_2\text{Se}_3$  [28].

The lower intensity peaks can be observed Cu2p and Se3d in XPS spectra of non-etched surface, while higher intensity of same spectra can be clearly observed on etched surface (Fig 3). On contrary, In3d in XPS spectra peaks are slightly more intense of non-etched surface as opposed to etched one. This is suggesting that concentration of Se and Cu is lowering  $\text{CuInSe}_2$  layer surface

as one of those elements in deeper layer of surface. In the meantime, the concentration of In is higher on the layer surface.

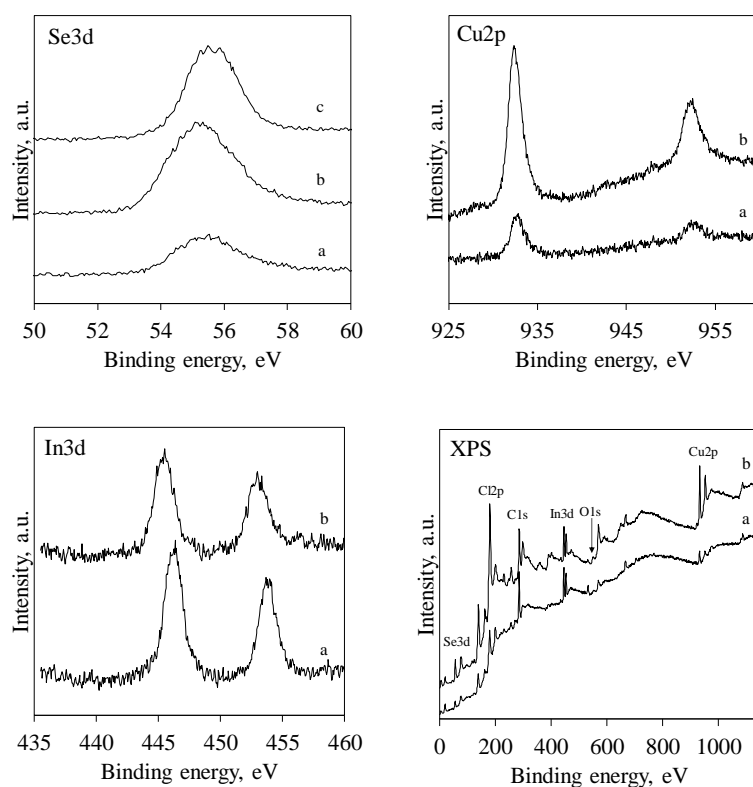


Fig. 2. High-resolution XPS spectra in  $\text{Se}3d_{5/2}$ ,  $\text{Cu}2p_{3/2}$  and  $\text{In}3d_{5/2}$  regions for Se and  $\text{CuInSe}_2$  layers prepared by SILAR method (a) as deposited layer, (b) annealed layer and (c) selenium layer.

Table 2. Atomic content of elements on the surface of  $\text{CuInSe}_2$  layer evaluated from XPS and atomic ratios of Cu/In and  $\text{Se}/(\text{Cu}+\text{In})$

Elements and atomic ratios	Atomic content, %	
	Not etched	After etching
Cu	4.02	16.07
In	7.11	8.41
Se	9.77	27.84
O	10.94	7.45
Cl	13.44	5.46
C	54.71	34.78
Cu/In	0.57	1.91
$\text{Se}/(\text{Cu}+\text{In})$	0.88	1.14

Some impurity elements such as O, Cl and C were also detected by XPS (Fig. 3, XPS). Among these elements, O is due to exposure to the atmosphere, and Cl is residual element from the precursor solution, C 1s of adventitious carbon is used as reference.

Composition analysis of  $\text{CuInSe}_2$  layer surface before and after etching is shown in Table 3. It is found out that in the surface of the  $\text{CuInSe}_2$  layer, the atomic ratio of Cu/In is about 0.57 which is lower than the atomic ratio of  $\text{Se}/(\text{Cu}+\text{In})$ . After the layer etching, the Cu/In ratio increased to 1.91 and became higher than  $\text{Se}/(\text{Cu}+\text{In})$  ratio although this ratio increased too from

0.88 to 1.14, which were probably caused due to sequence steps of layer forming. It is observed that composition becomes more uniform into the depth of the layer.

Based on the XPS results, it can be concluded that in the valence of Cu, In and Se in surface layer of and its depth up to 20  $\mu\text{m}$  were in form  $\text{CuInSe}_2$ ,  $\text{In}_2\text{Se}_3$  and  $\text{InCl}_3$  were  $\text{Cu}^{1+}$ ,  $\text{In}^{3+}$  and  $\text{Se}^{2-}$ , respectively.

From the analysis of XRD and XPS, we try to understand the reaction pathway of  $\text{CuInSe}_2$  layer deposited on SILAR method. It can be seen, that firstly, selenium layer was deposited that consists, mostly of red, amorphous selenium that has charge of  $\text{Se}^0$ . Next, layer is treated with solution, containing  $\text{Cu}^+$  ions, thus obtaining  $\text{Cu}_{0.87}\text{Se}$  phase. When this layer was exposed to solution containing  $\text{In}^{3+}$  ions, the XRD analysis had shown that compounds of  $\text{Cu}_{0.87}\text{Se}$  and  $\text{In}_2\text{Se}_3$  in the layer of  $\text{CuInSe}_2$  coexist. However, XPS analysis shows both  $\text{CuInSe}_2$ ,  $\text{In}_2\text{Se}_3$  and elemental Se are present in  $\text{CuInSe}_2$  layer. Copper selenide was not found due to (4), (5) and (6) reactions, because it remained deeper inside layer than 20  $\mu\text{m}$  XPS etching. Formed  $\text{CuInSe}_2$  and Se must be amorphous, because there were no XRD signals observed from freshly prepared layer. However, it is very likely that after annealing amorphous  $\text{CuInSe}_2$  and Se phase changes to crystalline cubic  $\text{CuInSe}_2$  and hexagonal Se, both are found using XRD analysis. Also, solid phase reactions (7) and (8) can take place and form same of on reaction (6). It can be seen, that order of  $\text{CuInSe}_2$  layer formation does influence deposited layer composition. In order to obtain homogeneous, crystalline  $\text{CuInSe}_2$  layer, it is necessary to anneal it in inert (nitrogen) atmosphere.

#### 4. Conclusions

$\text{CuInSe}_2$  layer on glass substrate was prepared in three steps by SILAR method and the composition of layer after each step has been studied. In addition, the effect of post-annealing treatment on the composition of this layer was studied. According to XRD analysis the formation sequence and the composition of  $\text{CuInSe}_2$  layer was Se (24-714) (Step 1)  $\rightarrow$   $\text{Cu}_{0.87}\text{Se}$  (83-1814) (Step 2)  $\rightarrow$   $\text{Cu}_{0.87}\text{Se}$  (83-1814),  $\text{In}_2\text{Se}_3$  (20-492) (Step 3)  $\rightarrow$   $\text{CuInSe}_2$  (23-207),  $\text{In}_2\text{Se}_3$  (17-356),  $\text{Cu}_{0.87}\text{Se}$  (83-1814), Se (73-465) (After annealing). Quantification of XPS peaks of Se3d, Cu2p and In3d confirms that after the third step formed phases of  $\text{CuInSe}_2$  and Se, which must be amorphous, because no XRD signals from this layer were observed. It is necessary to anneal in nitrogen atmosphere, in order to form  $\text{CuInSe}_2$  layer having a phase of crystalline  $\text{CuInSe}_2$ . The atomic ratios of Cu/In and Se/(Cu+In) on surface of  $\text{CuInSe}_2$  layer are 0.57 and 0.88 and they increasing with depth of layer (20  $\mu\text{m}$ ) from its surface accordingly up to 1.91 and 1.14. Based on experiment results, the possible reaction pathway of the layer of  $\text{CuInSe}_2$  on glass substrates synthesis procedure by SILAR method was proposed.

#### References

- [1] N. Kavcar, M.J. Carter, R. Hill, Sol. Energy Mater. Sol. Cells. 27 (1992).
- [2] J.C. Malaquias, M. Steichen, M. Thomassey, P.J. Dale, Electrochim. Acta. 103 (2013).
- [3] A.E.-H.B. Kashyout, E.-Z. Ahmed, T. Meaz, M. Nabil, M. Amer, Alexandria Eng. J. 53 (2014).
- [4] T. Tanaka, T. Yamaguchi, T. Ohshima, H. Itoh, A. Wakahara, A. Yoshida, Sol. Energy Mater. Sol. Cells. 75 (2003).
- [5] M.A. Green, K. Emery, Y. Hishikawa, W. Warta, E.D. Dunlop, Prog. Photovoltaics Res. Appl. 23 (2015).
- [6] J.-H. Park, M. Afzaal, M. Kemmler, P. O'Brien, D.J. Otway, J. Raftery, J. Mater. Chem. 13 (2003).
- [7] T. Suzuki, S. Ando, Semicond. Conf. (2015).
- [8] A. De Kergommeaux, A. Fiore, J. Faure-Vincent, A. Pron, P. Reiss, Adv. Nat. Sci. Nanosci. Nanotechnol. 4 (2013).
- [9] R. Chandran, R. Pandey, A. Mallik, Mater. Lett. 160 (2015).

- [10] M. Berruet, Y. Di Iorio, M. Troviano, M. Vázquez, *Mater. Chem. Phys.* 148 (2014).
- [11] J.F. Han, C. Liao, E. Gautron, T. Jiang, H.M. Xie, K. Zhao, *Vacuum*. 105 (2014).
- [12] C.-H. Shih, I. Lo, S.-T. You, C.-D. Tsai, B.-H. Tseng, Y.-F. Chen, *Thin Solid Films*. 574 (2015).
- [13] H. Abdullah, S. Habibi, *Int. J. Photoenergy*, 2013 (2013).
- [14] Z.H. Li, E.S. Cho, S.J. Kwon, M. Dagenais, *J. Mater. Sci. Mater. Electron.* 23 (2012).
- [15] A.E. Zaghi, M. Buffiere, G. Brammertz, N. Lenaers, M. Meuris, J. Poortmans, *Thin Solid Films*. 582 (2015).
- [16] A.E. Zaghi, M. Buffiere, G. Brammertz, M. Batuk, N. Lenaers, B. Kniknie, *Adv. Powder Technol.* 25 (2014).
- [17] V. Zelionkaitė, A. Žarnauskas, *Chem. Technol.* 18 (2001).
- [18] J. Sukyte, A. Ivanauskas, I. Ancutiene, *Chalcogenide Lett.* 12 (2015).
- [19] Р.А. Лидин, В.А. Молочко, Л.Л. Андреева, *Справочник по неорганической химии*, 1987.
- [20] R. Zingaro, C. Cooper, *Selenium*, 1973.
- [21] G. Malmsten, I. Thoren, S. Hogberg, J. Bergmark, S. Karlsson, E. Rebane, *Phys. Scr.* 3 (1971).
- [22] P.E. Sobol, A.J. Nelson, C.R. Schwerdtfeger, W.F. Stickle, J.F. Moulder, *Surf. Sci. Spectra*. 1 (1992).
- [23] G. Ertl, R. Hierl, H. Knözinger, N. Thiele, H.P. Urbach, *Appl. Surf. Sci.* 5 (1980).
- [24] J.G. Jolley, G.G. Geesey, M.R. Hankins, R.B. Wright, P.L. Wichlacz, *Appl. Surf. Sci.* 37 (1989).
- [25] D. Cahen, P.J. Ireland, L.L. Kazmerski, F.A. Thiel, *J. Appl. Phys.* 57 (1985).
- [26] Freeland B.H., Habeeb J.J., Tuck D.G., *Can. J. Chem.* 55, 1528 (1977)
- [27] G. Sakane, T. Shibahara, *Inorg. Chem.* 32 (1993).
- [28] L.L. Kazmerski, O. Jamjoum, P.J. Ireland, S.K. Deb, R.A. Mickelsen, W. Chen, *J. Vac. Sci. Technol.* 19 (1981).